AN ASSESSMENT OF SPHERE DRAG COEFFICIENT DATA

By Helmut G. Heinrich and Robert A. Noreen

University of Minnesota

INTRODUCTION

In order to reliably determine atmospheric conditions from the descent velocity of a sphere, the drag coefficient of the sphere as it falls through the air must be known to a high degree of accuracy. This paper covers wind tunnel studies which established drag coefficients from 360,000 ft. altitude down for a one meter sphere with a given weight, when ejected from a rocket at an altitude of 450,000 ft. The wind tunnel test conditions were adjusted for simultaneous duplication of the Mach and Reynolds Numbers as they occur during the descent of the sphere in a standard atmosphere. The range of the test conditions was wide enough to cover the expected atmospheric deviations.

TEST FACILITIES

The drag coefficient of a perfect sphere moving through air is a function of the Mach and Reynolds Numbers and under certain conditions also of the Knudson Number which is, however, a combination of Mach and Reynolds Numbers. These relationships require that meaningful drag measurements must be made with simultaneous duplication of the respective Mach and Reynolds Numbers. In standard atmospheric pressure wind tunnels, this condition is usually difficult to fulfill. Therefore, the University of Minnesota used for the required measurements a subsonic and a supersonic variable density wind tunnel, because the density variation provides the third parameter necessary to establish the required Mach-Reynolds and Knudson Number simulation.

The low density subsonic wind tunnel is of the closed horizontal return type, Fig. 1 (Ref. 1), with a mechanical vacuum pump used to evacuate the circuit and a centrifugal compressor to move the air around the circuit. Continuous operation at Mach Numbers from nearly 0 up to approximately 0.9 can be obtained by using various nozzles and a throttling valve. Wind tunnel operating

pressures range from 200 torr down to approximately 0.2 torr, depending upon the flow Mach Number. The nozzles exhaust into an open jet test section and have outlet diameters varying from 12 in. for lowest Mach Numbers to 3 in. for highest Mach Numbers.

The low density supersonic wind tunnel, Fig. 2 (Ref. 2), has a standard "blow down" configuration, operating between a 5000 psig high pressure source and a 10 millitorr vacuum reservoir. For these tests the supersonic wind tunnel was equipped with five axisymmetric nozzles for operation at Mach Numbers of 1.2, 1.5, 2.0, 2.5, and 3.2 at static pressures in the order of 1 torr. All five nozzles have a core flow region 4 in. in diameter at their design operating pressures and exhaust into an open jet test section. For the pressures of interest in the sphere drag tests, the 33,500 cu. ft. vacuum reservoir could sustain nearly constant pressures for run times of a minute or longer.

MODELS

The sphere models used in both test sequences were 0.50 in. Teflon spheres with diameter tolerances of 0.002 in. and sphericity of 0.001. Teflon was selected because its surface roughness characteristics approximate those of an inflated spherical Mylar balloon.

MEASUREMENTS

The primary measurements made during the tests were flow pressures and the drag forces of the spheres. Naturally the size of the models and flow temperature were also measured, but these measurements presented little or no difficulty and could be made with sufficient accuracy to be neglected in an error analysis.

The pressure measurements in the required range from 20 torr to 10 millitorr presented the most difficulties and created the largest portion of the total error. For both the subsonic and supersonic tests measuring two pressures enabled determing the flow conditions. In the subsonic tests, total pressure and the difference between total and static pressure were measured, while in the supersonic tests, total pressure and static pressure were determined. These measurements were made using Bourdon tube, strain-gaged diaphragm, and thermocouple gages, all having different ranges, accuracies, and reliabilities (Refs. 1 and 2). Total pressures were detected with a total probe rake located in a near stagnation region, and static pressures were obtained from static pressure taps in the nozzle wall near the exit.

Drag forces were measured using the force balance shown in Fig. 3. A drag force acting on the sphere twists the torsion member causing the core of a linear variable differential transformer to deflect within the coil, thus producing a measurable change in coil current. Two permanent magnets placed near a copper "paddle", also attached to the torsion member, produced sufficient eddy currents to damp any oscillation of the balance system. The balance was calibrated by hanging weights on the damping support strut and relating the moment produced by the weight to a force on the sphere by the ratios of lengths to the moment center. Changing torsion members allowed selecting nearly any required sensitivity of the force balance. Repeated calibrations indicated that the balance performed quite well and was more accurate than the electrical read-out equipment used to measure the coil currents.

For each data point two types of drag measurements were made, one with the sphere mounted on its sting support, and another one of the support alone with the sphere rigidly mounted slightly ahead of the support (Fig. 4). Subtracting the support drag from the total drag yielded the drag of the sphere. The drag of the support was, of course, considerably smaller than that of the sphere.

RESULTS

The results from the supersonic and subsonic tests are shown in Figs. 5 and 6, respectively, as plots of drag coefficient vs Reynolds Number with Mach Number as a parameter. One notices that the higher speed subsonic data is somewhat scattered and that there are a few questionable points among the supersonic results. In view of this uncertainty, the data was replotted in Figs. 7a and 7b as C_D vs Mach Number with Reynolds Number as parameter. The critical review of both types of presentations provides guide lines for the data interpretation and for the establishment of the final conclusion. In this view, the data in the previous figures was carefully analyzed by members of the staff of the University of Minnesota and USAF Cambridge Research Laboratories. The results of this joint effort are the curves shown in Figs. 8 and 9 which are considered to be the final results of this study. The two dashed curves in Fig. 8 show the spread of data obtained at Mach Numbers between 2 and 4 in wind tunnel tests by Ashkenas who performed wind tunnel tests with spheres mounted on thin wires (Ref. 3).

The agreement between the different supersonic data can only be termed approximate at best, and even though Ashkenas (Ref. 3) presents no error estimate, there is no principal reason that accurate results could not be obtained with his methods.

Figure 9 includes several data points from tests conducted with moving spheres in a ballistic range (Ref. 4). The agreement between these data is again approximate, and not within the estimated error range of either set of measurements. However, it is not known if drag measurements taken from a sphere which is decelerating to various degrees as it travels along the ballistic range can be compared to steady state measurements. In a flow field that changes with time, the flow pattern may be quite different from the one under steady state conditions at the same Mach and Reynolds Numbers. The kinetic energy in that flow field varies definitely, and apparent mass effects may have to be accounted for. Therefore, it is at this time not known if these effects involved in the ballistic tests are or are not significant, but it is a possible explanation for the difference between results obtained under steady state and non-steady conditions.

ERRORS

References 1 and 2 give extended analyses of the random and instrument errors encountered in the measurements performed at the University of Minnesota. The analysis follows the standard concept of expressing the error in drag coefficient as a total differential considering all the terms measured to obtain the drag coefficient. The results of this analysis predict errors from 1% to 5% for the subsonic measurements, and from 2% to 28% for the supersonic measurements; these numbers represent the maximum possible errors due to random or instrument errors, and the possible error for a particular point is a function of the Mach and Reynolds Number at that point. For both the subsonic and supersonic data, the highest errors occur at the lowest Reynolds Numbers of the range, and in both cases, the highest possible error is due to the pressure error term.

CONCLUSIONS

Sphere drag coefficients have been measured over the range of Mach and Reynolds Numbers encountered by a falling sphere density sensor. An error analysis of the data shows that generally the data should be accurate to within about 5%; agreement with other measurements is within about 10% and results from actual tests show that the data is at worst very reasonable and at best highly accurate. Of course, since the drag coefficient data is one basic part of a measuring system where greater and greater accuracy is needed, the drag coefficients must be critically checked for possible inaccuracy and improvement. Reviewing the measurements from this aspect, several possible areas for improvement arise.

1. Pressure Measurement

Since the measurements were conducted fairly significant improvements in pressure measuring instrumentation and techniques have been made. Realizing that the highest errors in the data presented above were no doubt caused by pressure errors, it seems probable that at least in some ranges significant improvements could be made in the accuracy of the coefficients.

2. Sphere Temperature

Recent publications have shown that sphere temperature does have an influence on drag coefficients in this low density flow regime (Ref. 5). Although this effect is not large and the model spheres should have been at a temperature very near wall temperature, the sphere temperature was not measured. If temperature differences existed, this may have caused some unknown error.

3. Sphere Surface Roughness

Only one type of sphere was used in the tests at the University of Minnesota, hence the effects of roughness were not determined experimentally. It is possible that at least part of the deviation from measurements at other institutions is due to different surface roughness of the models.

SUMMARY

It appears that the drag of the sphere is known reasonably well with an accuracy usually expected from aerodynamic measurements. Yet an over-all improvement of the accuracy of the pressure sensing system offers greater certainty in the process of data acquisition and probably a significant improvement of the accuracy of the drag coefficients.

A new effort to measure the sphere drag under well simulated steady state flow conditions with the best instrumentation and facilities available appears to be justified and desirable.

ADDENDUM

During the discussion following this and other presented papers, questions were raised about the origin of the $M \leqq 0.39$ sphere drag coefficient data between Reynolds Numbers of 1,600 and 25,000 presented in Ref. 1. The uncertainties center around Fig. 19 of Ref. 1, added here as Fig. 10, which shows the results of measurements by the University of Minnesota. All of the data in Fig. 10, except the $M \leqq 0.39$ data, has been superseded by the data shown in Fig. 9 (Ref. 2), which were obtained from tests conducted with better instrumentation at a later date. The drag coefficients shown in Fig. 10 and identified as belonging to Mach Number $\leqq 0.39$ have not been changed because newer test cases with improved instrumentation did not show significant deviations from the earlier established data.

The $M \leqq 0.39$ curve is based on seven series of measurements at various Mach Numbers between Reynolds Numbers of 1.5×10^3 to 3×10^4. This is also stated in Ref. 1. Detailed results of these measurements are shown in Fig. 11. The data points presented in Fig. 11 were not shown in Fig. 19 of Ref. 1 in order to avoid overcrowding the presentation.

Figure 10 shows an additional curve representing drag coefficients in the incompressible flow regime for Reynolds Numbers less than 10^3. This information is taken from Fig. 10 in Chapter III of Hoerner's "Fluid-Dynamic Drag," as well as a graphical transposition can be made. Admittedly, Fig. 19, Ref. 1, can easily be misunderstood to the extent that the entire curve representing the sphere drag coefficients in the incompressible range is credited to Hoerner. This is, however, not true and the right-hand segment represents the average values shown in Fig. 11. Merely the left-hand portion is from Hoerner.

Comparing the University of Minnesota curve $M \leqq 0.39$, one finds as minimum drag coefficient $C_D = 0.427$ for Reynolds Numbers between 3.5 and 4.0×10^3. Trying to extract the minimum C_D value from Hoerner's curve one finds for the same Reynolds Number range $C_D = 0.407$ with a possible reading inaccuracy of ± 0.025. This fact led to the remark in Ref. 1 that the University of Minnesota measured data agree well with Hoerner's curve covering this Reynolds Number range.

Furthermore, it will be noticed that Fig. 11 also contains data points taken from numerical values of Ref. 6, which is one publication listed in Hoerner. Figure 12 is a photographic reproduction of Fig. 26, Ref. 6.

This figure is particularly interesting since it shows different drag coefficients for the same Reynolds Numbers obtained by a different experimental technique, namely dropping steel spheres in water.

Figure 13 which is reproduced from Ref. 7, Fig. 178, is also included and shows the variation of drag coefficients measured in the same institution under the supervision of the same individuals but in different wind tunnels. Of course, it must be considered that Fig. 13 shows the drag coefficients in the

critical subsonic range, and the degree of wind-tunnel turbulence is in this region particularly influential.

Summarizing then all matters of accuracy, it is the opinion of these authors that the accuracy of the drag coefficients measured at the University of Minnesota is about as good as can be expected from wind-tunnel experiments at that time. Repeating these measurements and utilizing instrumentation improved over that available in 1960 to 1962 may provide somewhat different results, but the deviations cannot be large. Furthermore, different measuring techniques such as measuring the descent speed of spheres in water or their deceleration in a ballistic range may again produce slightly different numerical values.

REFERENCES

1. Heinrich, Helmut G.; Niccum, Ronald J.; and Haak, Eugene L.: The Drag Coefficient of a Sphere Corresponding to a "One Meter ROBIN Sphere" Descending From 260,000 ft Altitude (Reynolds Nos 789 to 23,448, Mach Nos 0.056 to 0.90). Research and Development of ROBIN Meteorological Rocket Balloon, Vol. II, Contract No. AF 19(604)-8034, Univ. of Minnesota, May 1963. (Available from DDC as AD 480309.)

2. Heinrich, H. G.; Niccum, R. J.; Haak, E. L.; Jamison, L. R.; and George, R. L.: Modification of the Robin Meteorological Balloon. Vol. II - Drag Evaluations. AFCRL-65-734(II), U.S. Air Force, Sept. 30, 1965. (Available from DDC as AD 629775.)

3. Ashkenas, H. I.: Sphere Drag at Low Reynolds Numbers and Supersonic Speeds. Res. Summary No. 36-12, Vol. I (Contract No. NAS 7-100), Jet Propulsion Lab., California Inst. Technol., Jan. 2, 1962, pp. 93-95.

4. Lawrence, W. R.: Free-Flight Range Measurements of Sphere Drag at Low Reynolds Numbers and Low Mach Numbers. AEDC-TR-67-218, U.S. Air Force, Nov. 1967. (Available from DDC as AD 660545.)

5. Ashkenas, Harry: Low-Density Sphere Drag With Equilibrium and Nonequilibrium Wall Temperature. Rarefied Gas Dynamics, Vol. II, J. A. Laurmann, ed., Academic Press, 1963, pp. 278-290.

6. Ergebnisse der Aerodynamischen Versuchsanstalt zu Goettingen. II. Lieferung, Verlag von R. Oldenbourg, 1923, pp. 28-30.

7. Ergebnisse der Aerodynamischen Versuchsanstalt zu Goettingen. IV. Lieferung, Verlag von R. Oldenbourg, 1932, pp. 106-108.

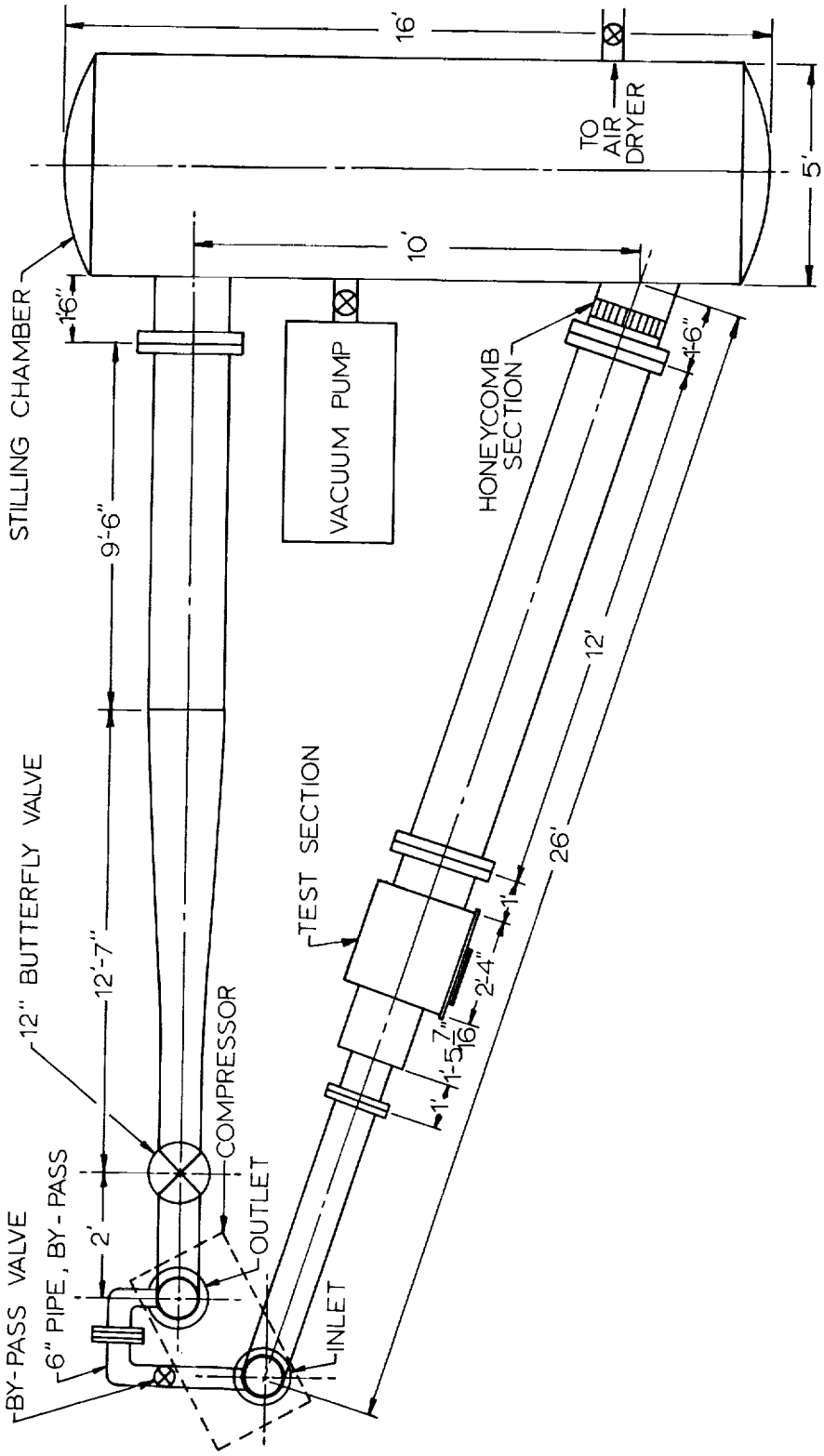

Figure 1.- Low density wind tunnel layout.

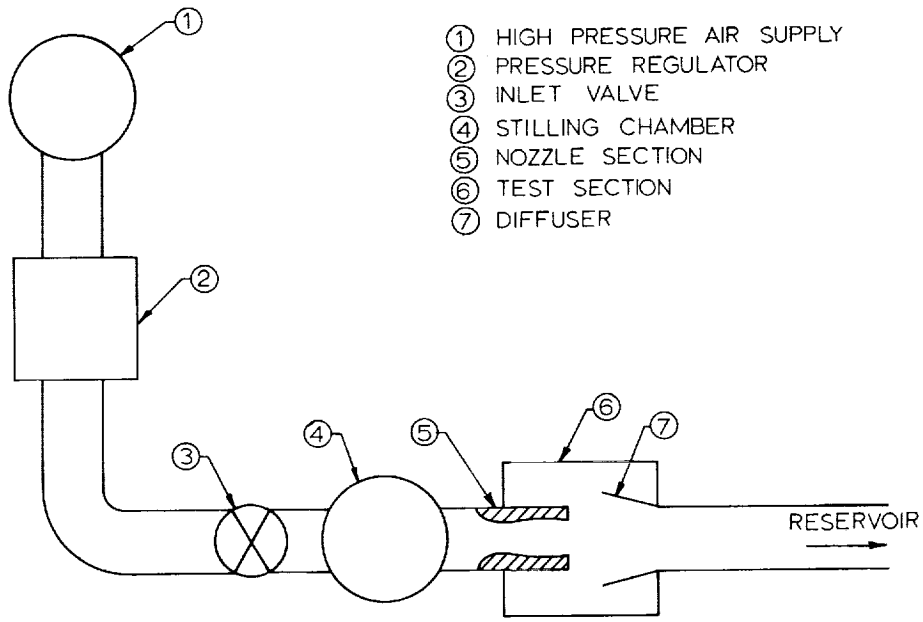

Figure 2.- Schematic representation of the low density supersonic wind tunnel.

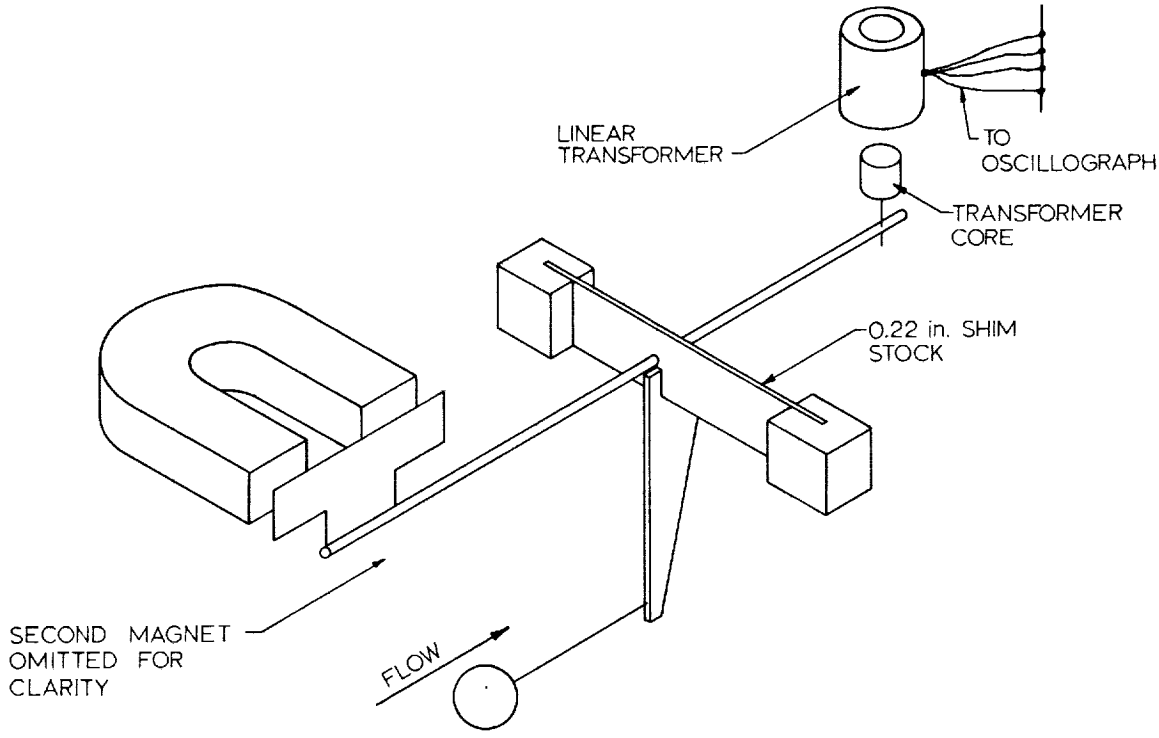

Figure 3.- Schematic of drag balance used in low density supersonic wind tunnel.

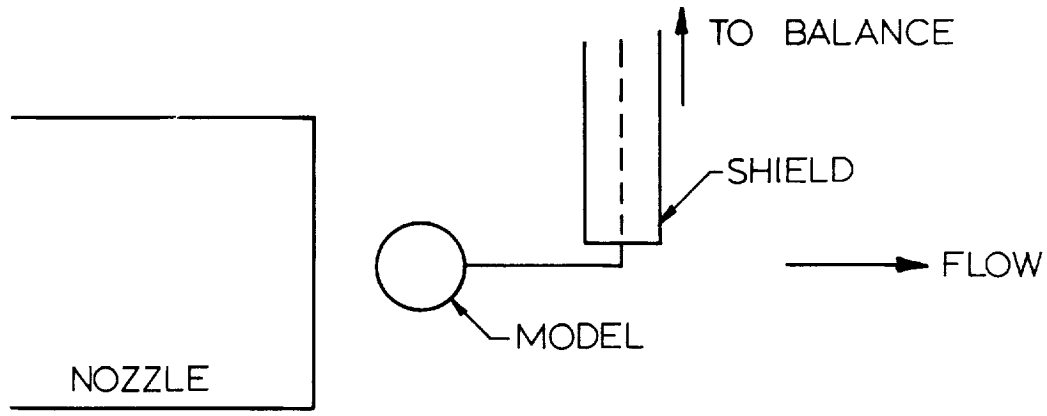

(a) Total force arrangement.

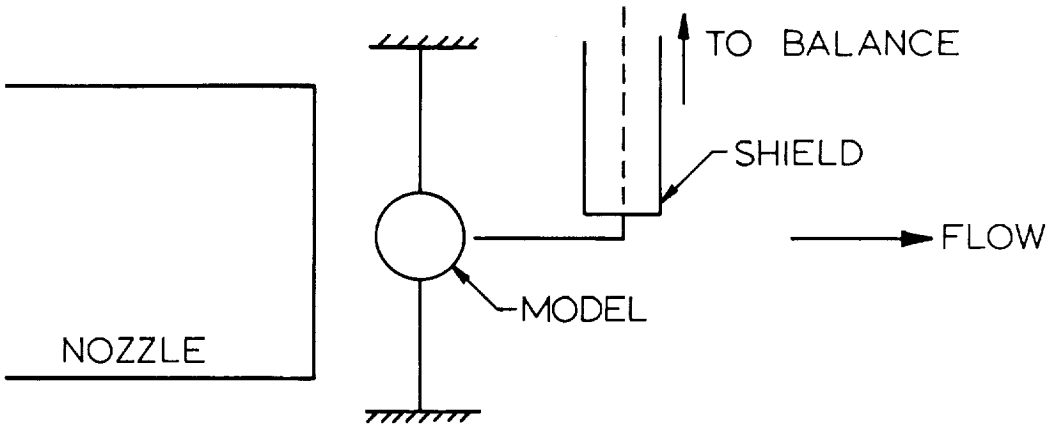

(b) Tare force arrangement.

Figure 4.- Schematic representation of suspension arrangement for force measurements.

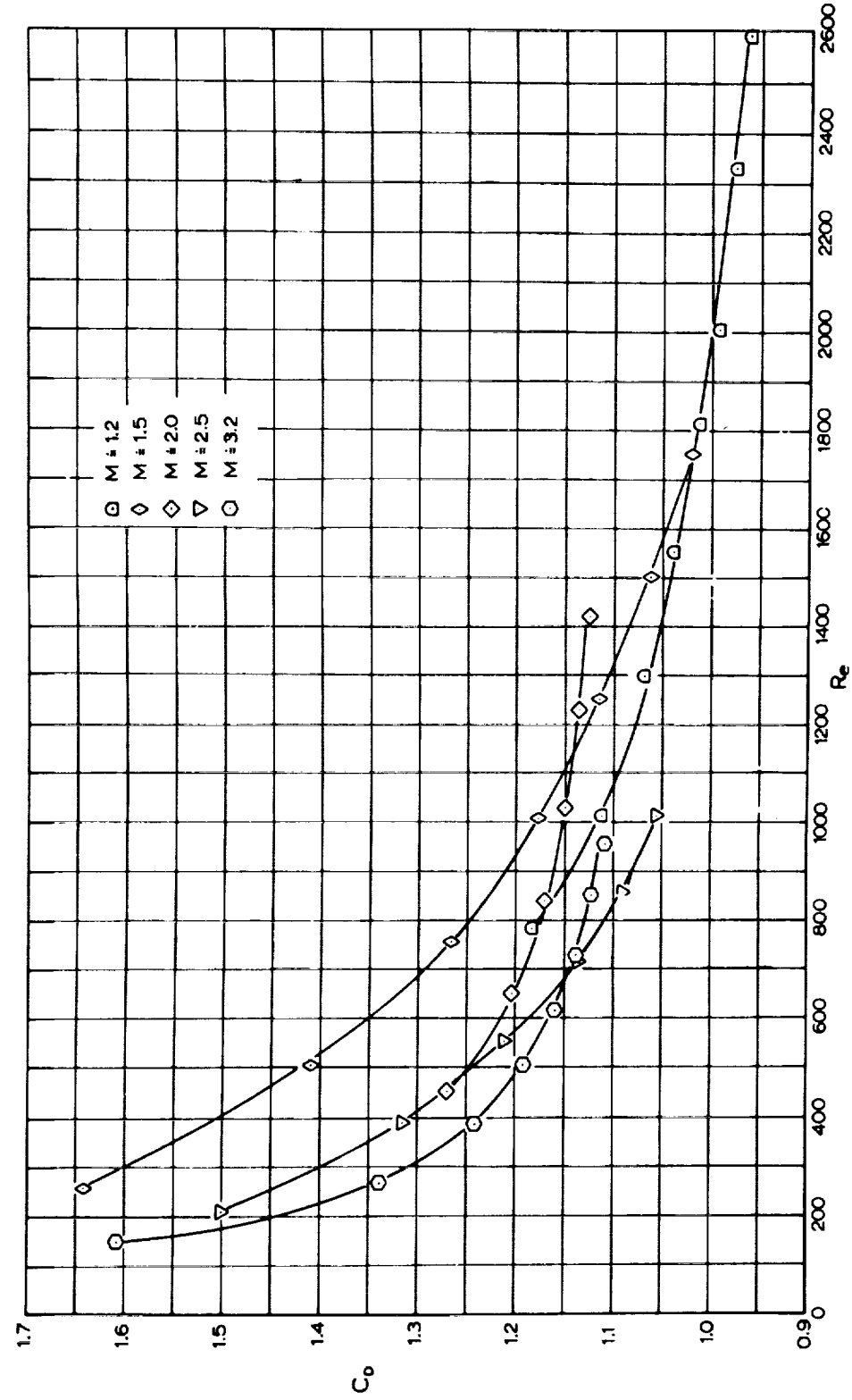

Figure 5.- Drag coefficient of a sphere in supersonic flow as a function of the free-stream Reynolds number.

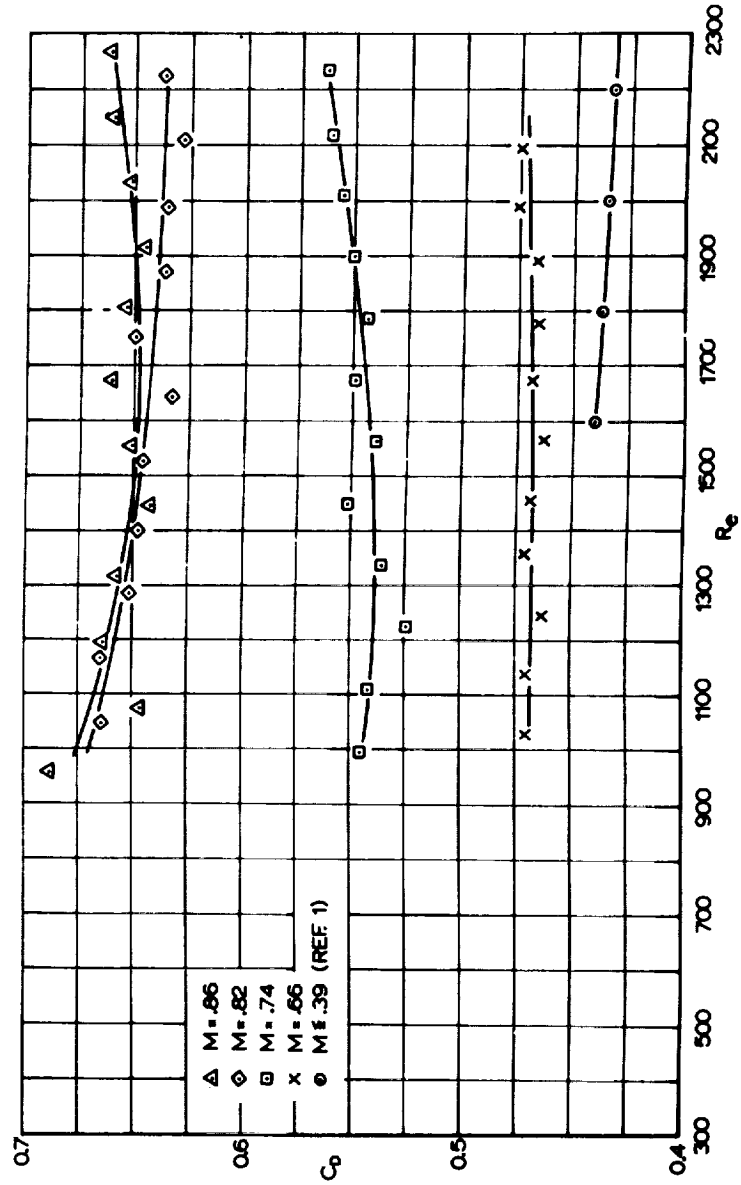

Figure 6.- Drag coefficient of a sphere in subsonic flow as a function of the free-stream Reynolds number.

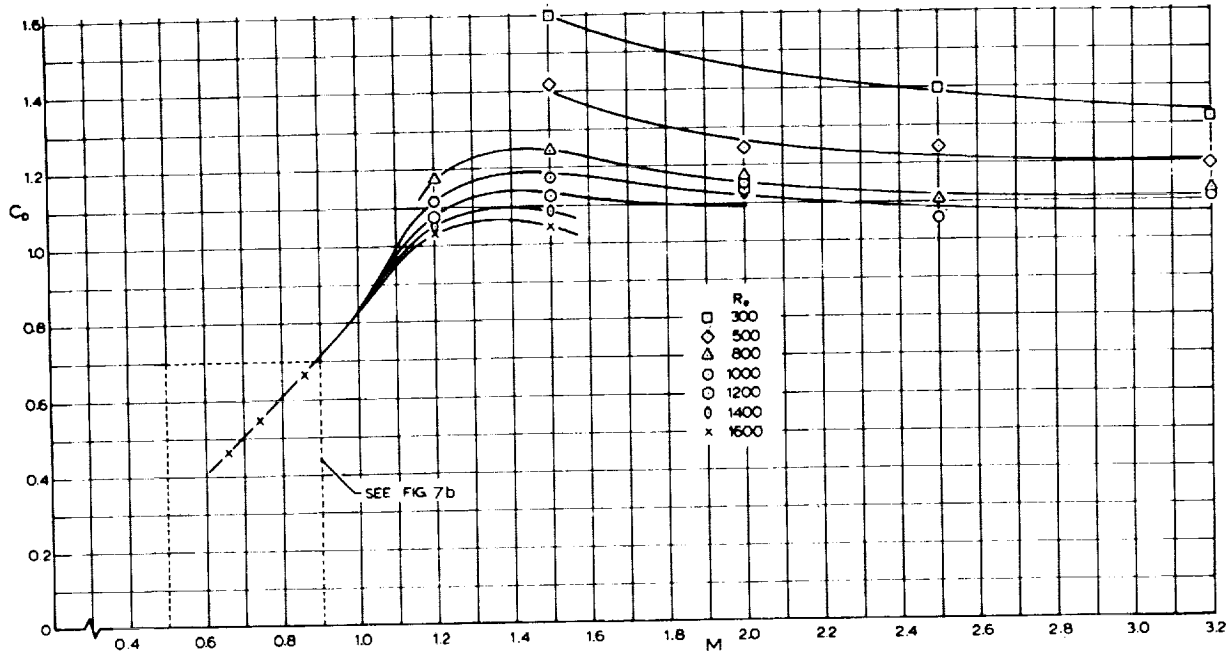

(a) $0.66 \leq M \leq 3.2$.

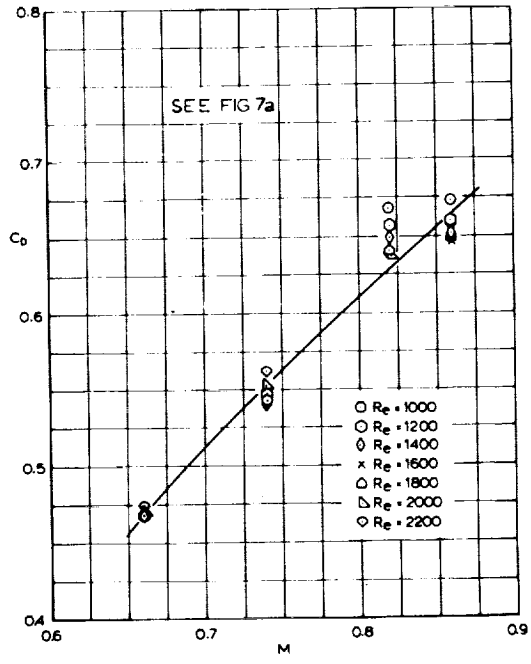

(b) $0.66 \leq M \leq 0.86$.

Figure 7.- Drag coefficient of a sphere as a function of the free-stream Mach number with Reynolds number as a parameter.

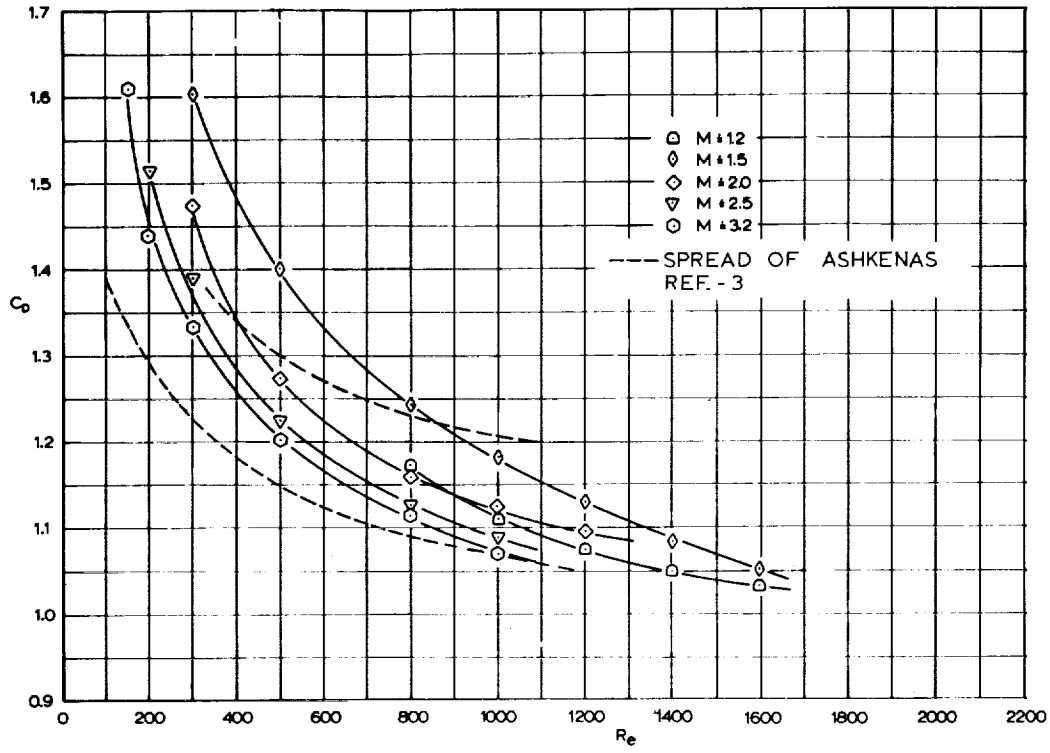

Figure 8.- Drag coefficient of a sphere in supersonic flow as a function of the free-stream Reynolds number.

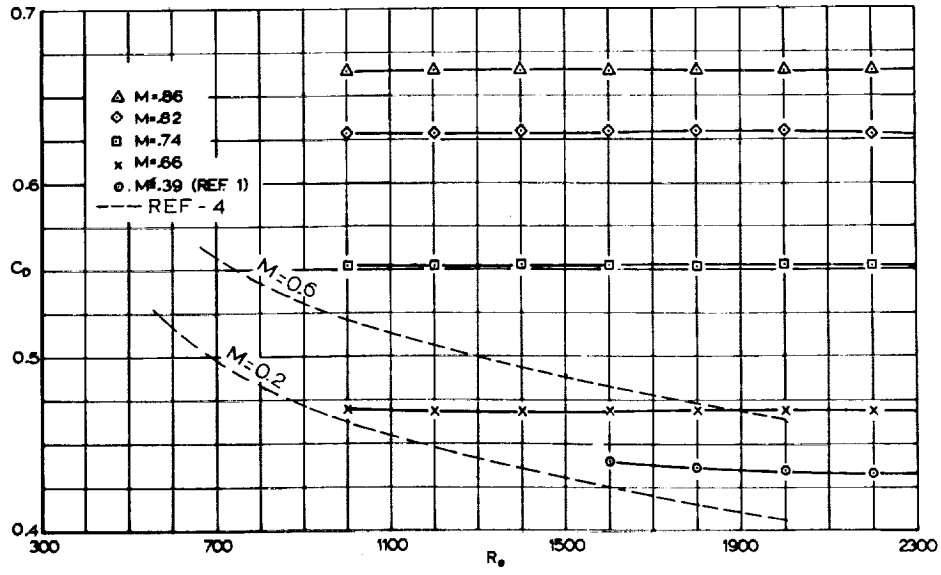

Figure 9.- Drag coefficient of a sphere in subsonic flow as a function of the free-stream Reynolds number.

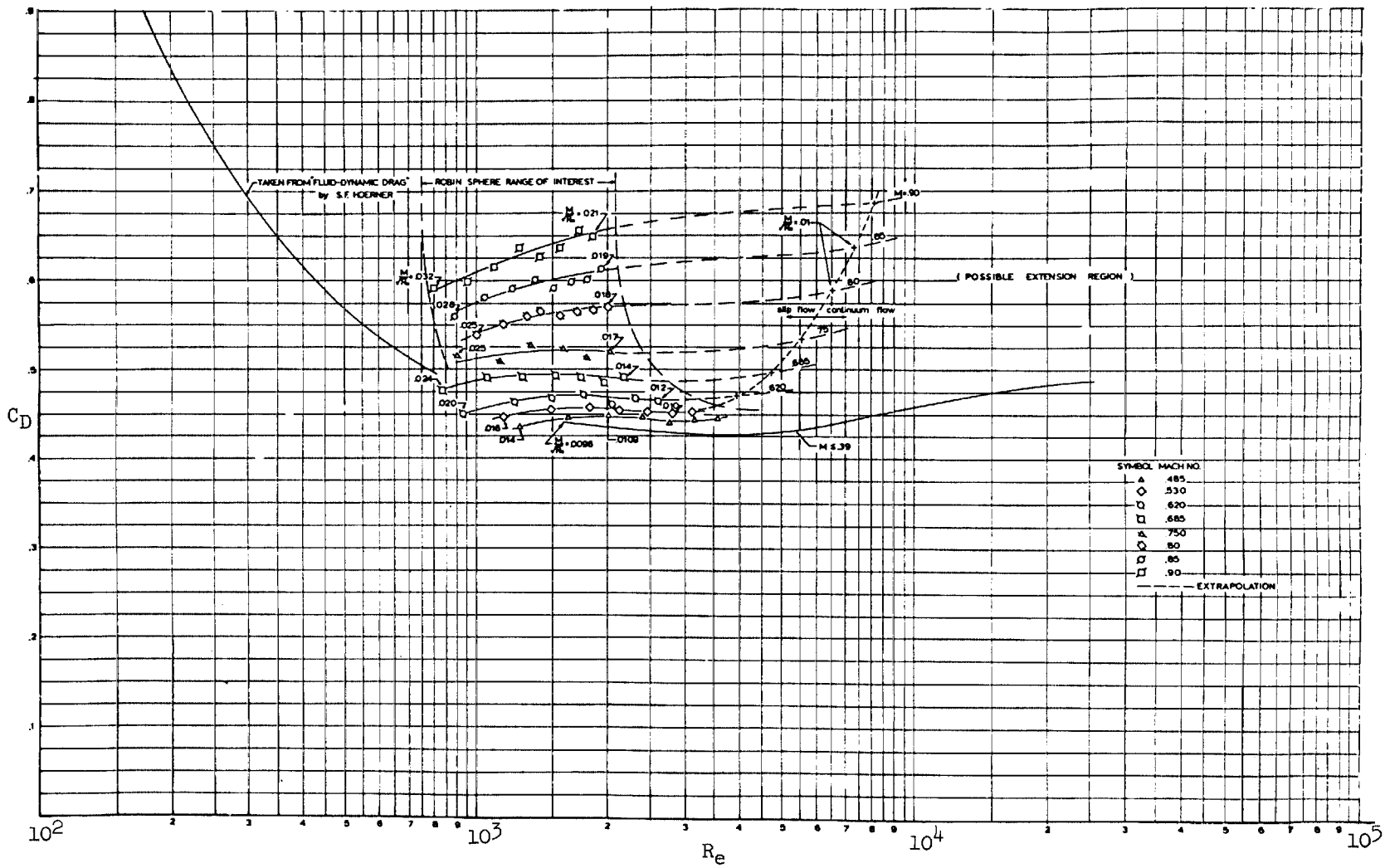

Figure 10.- Drag coefficients of a sphere at various Reynolds Numbers in subsonic flow (taken from Ref. 1, Fig. 19).

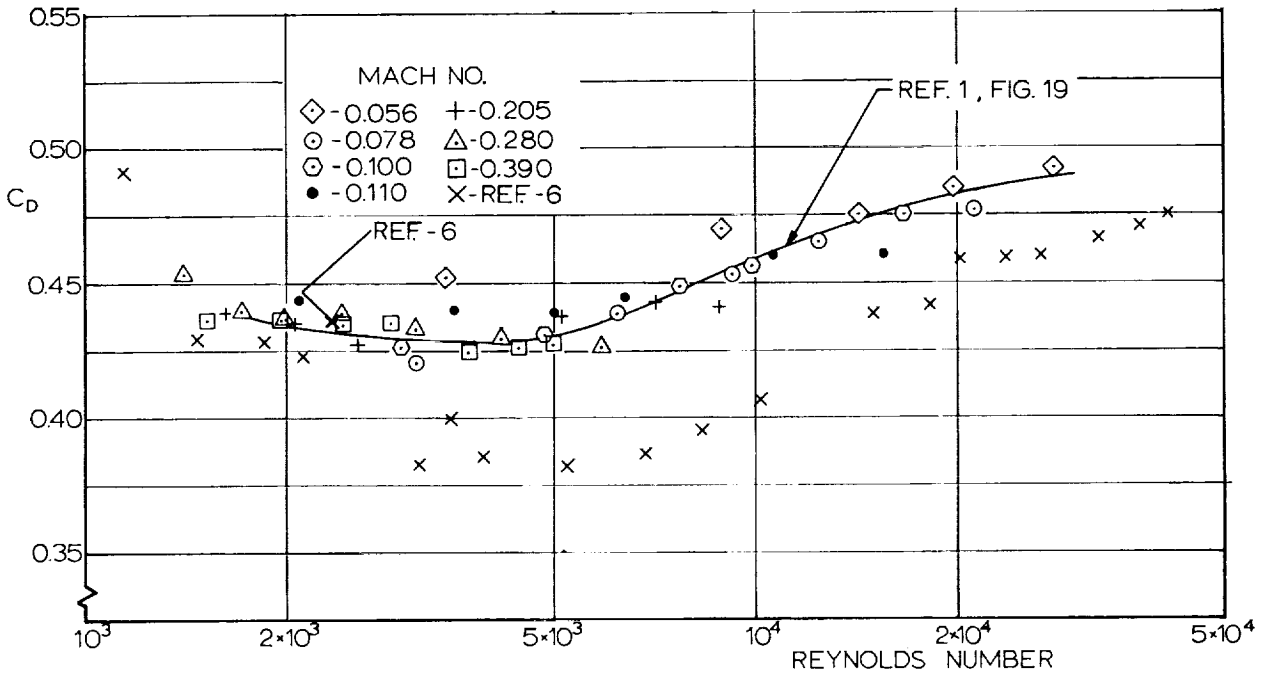

Figure 11.- Low subsonic drag coefficients measured at University of Minnesota compared with data taken from Ref. 6.

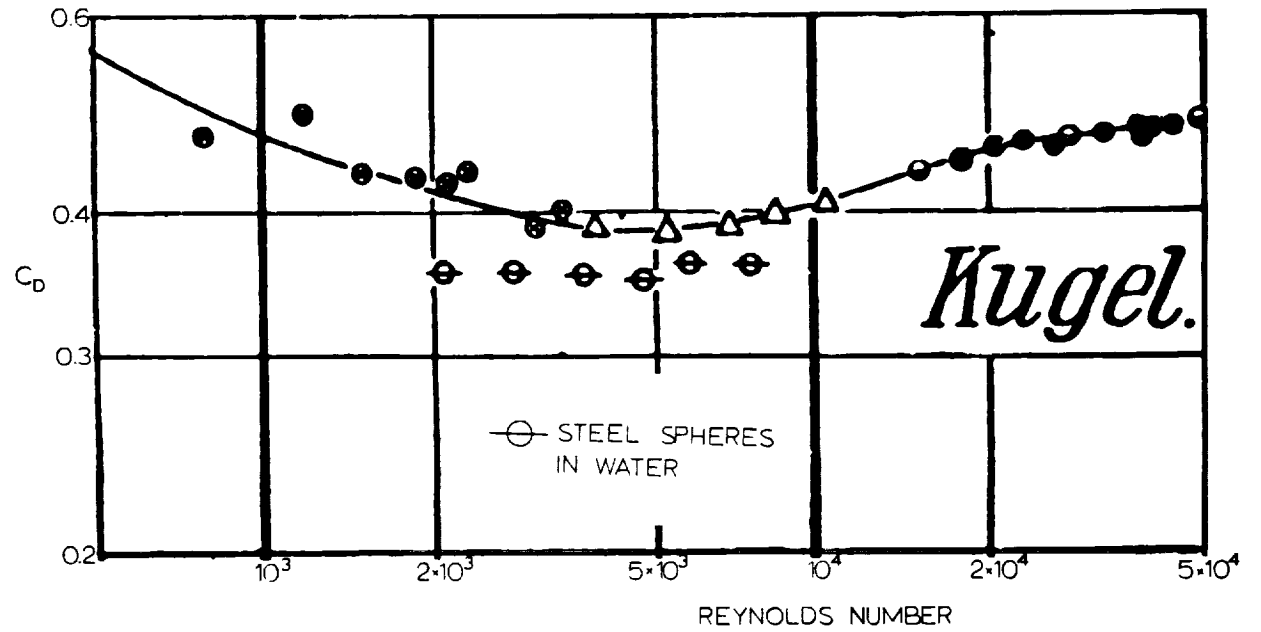

Figure 12.- Drag coefficients of a sphere in subsonic flow at Reynolds Number between 10^3 to 5×10^4. (Reproduced from Ref. 6.)

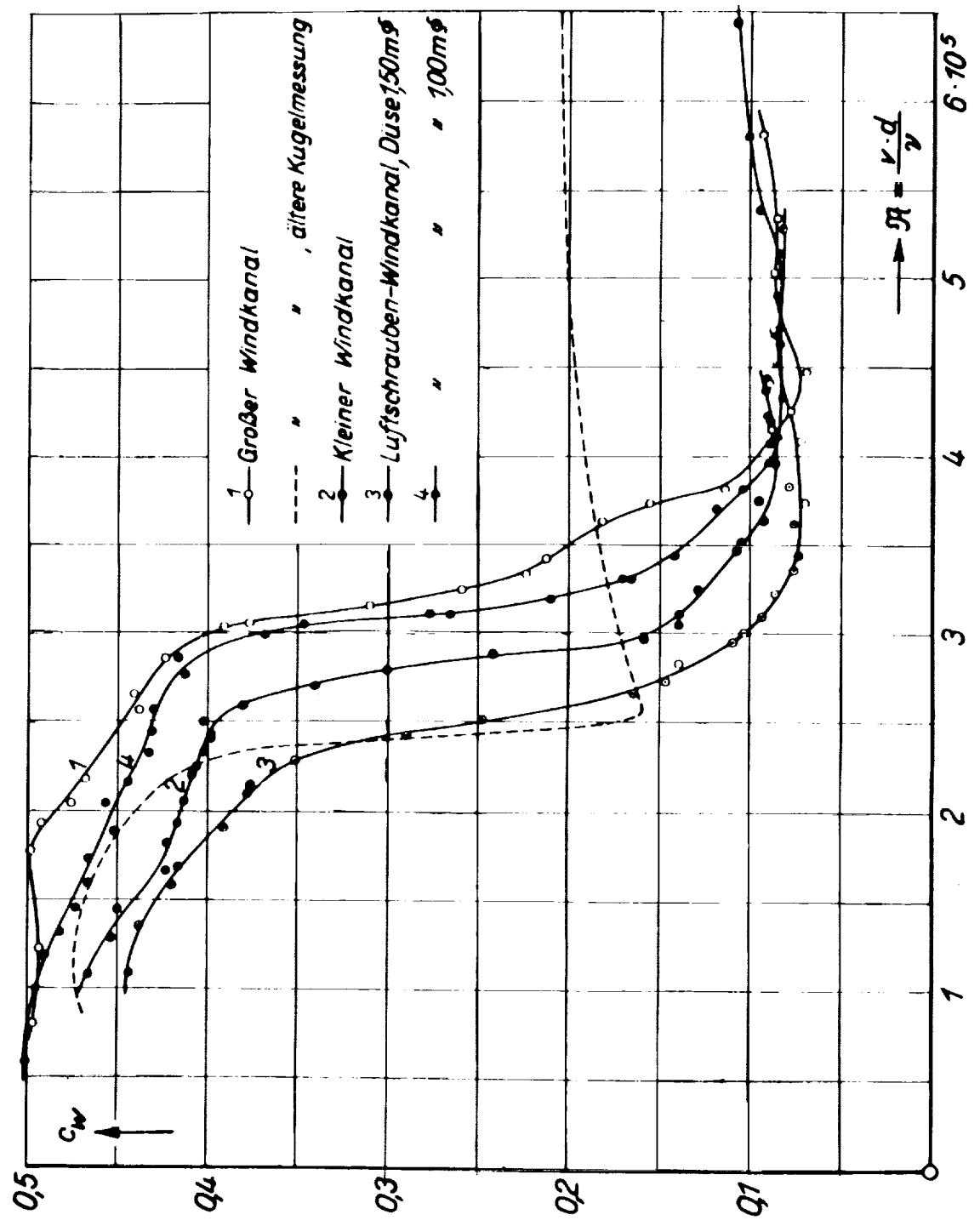

Figure 13.- Drag coefficients of a sphere in subsonic flow in the critical range measured in different windtunnels. (Reproduced from Ref. 7.)